

Kartogenin Enhances Collagen Organization and Mechanical Strength of the Repaired Enthesis in a Murine Model of Rotator Cuff Repair



Dean Wang, M.D., Hongbo Tan, M.D., Ph.D., Amir H. Lebaschi, M.D.,
Yusuke Nakagawa, M.D., Ph.D., Susumu Wada, M.D., Ph.D., Patrick E. Donnelly, Ph.D.,
Liang Ying, B.S., Xiang-Hua Deng, M.D., and Scott A. Rodeo, M.D.

Purpose: To investigate the use of kartogenin (KGN) in augmenting healing of the repaired enthesis after rotator cuff repair in a murine model. **Methods:** Seventy-two C57BL/6 wild-type mice underwent unilateral detachment and transosseous repair of the supraspinatus tendon augmented with either fibrin sealant (control group; n = 36) or fibrin sealant containing 100 $\mu\text{mol/L}$ of KGN (experimental group; n = 36) applied at the repair site. Postoperatively, mice were allowed free cage activity without immobilization. Mice were humanely killed at 2 and 4 weeks postoperatively. Repair site integrity was evaluated histologically through fibrocartilage formation and collagen fiber organization and biomechanically through load-to-failure testing of the supraspinatus tendon–bone construct. **Results:** At 2 weeks, no differences were noted in percent area of fibrocartilage, collagen organization, or ultimate strength between groups. At 4 weeks, superior collagen fiber organization (based on collagen birefringence [17.3 ± 2.0 vs 7.0 ± 6.5 integrated density/ μm^2 ; $P < .01$]) and higher ultimate failure loads (3.5 ± 0.6 N vs 2.3 ± 1.1 N; $P = .04$) were seen in the KGN group. The percent area of fibrocartilage ($13.2 \pm 8.4\%$ vs $4.4 \pm 5.4\%$; $P = .04$) was higher in the control group compared with the KGN group. **Conclusions:** Rotator cuff repair augmentation with KGN improved the collagen fiber organization and biomechanical strength of the tendon–bone interface at 4 weeks in a murine model. **Clinical Relevance:** These findings have implications for improving the structural integrity of the repaired enthesis and potentially reducing the retear rate after rotator cuff repair, which can ultimately lead to improvements in clinical outcomes.

See commentary on page 2588

The healing of the surgically repaired rotator cuff tendon to the bone remains one of the biggest challenges in orthopaedics, with reported retearing or

nonhealing rates of 10% to 28% for medium to large tears.¹ This is in part due to the inability of natural physiologic healing to recreate the transitional 4-zone interface of the native fibrocartilaginous enthesis. Rather, the tendon heals to bone through a fibrovascular scar tissue, which has inferior biomechanical properties compared with the native enthesis, making the construct susceptible to failure.^{2,3} The native enthesis is divided into 4 zones with increasing stiffness: tendon, nonmineralized fibrocartilage, mineralized fibrocartilage, and bone. Dissipation of force is achieved effectively through this gradual transition from tendon to fibrocartilage to bone.⁴

Attempts to regenerate the zonal structure of this native fibrocartilaginous enthesis, either with graded scaffolds, bioactive agents, and stem cells, has thus far been met with limited success.⁵ Kartogenin (KGN), a small synthetic heterocyclic compound (Fig 1), has been reported to induce chondrogenic differentiation of

From the Sports Medicine and Shoulder Service (D.W., S.A.R.), and the Laboratory for Joint Tissue Repair and Regeneration (D.W., H.T., A.H.L., Y.N., S.W., P.E.D., L.Y., X-H.D., S.A.R.), Hospital for Special Surgery, New York, New York, U.S.A.

The authors report that they have no conflicts of interest in the authorship and publication of this article. Full ICMJE author disclosure forms are available for this article online, as [supplementary material](#).

Investigation performed at the Hospital for Special Surgery, New York, New York, U.S.A.

Paper presented at the American Academy of Orthopaedic Surgeons Annual Meeting, March 6-10, 2018, New Orleans, Louisiana.

Received January 31, 2018; accepted April 24, 2018.

Address correspondence to Dean Wang, M.D., 535 East 70th Street, New York, New York 10021, U.S.A. E-mail: deanwangmd@gmail.com

© 2018 by the Arthroscopy Association of North America
0749-8063/18136/\$36.00

<https://doi.org/10.1016/j.arthro.2018.04.022>

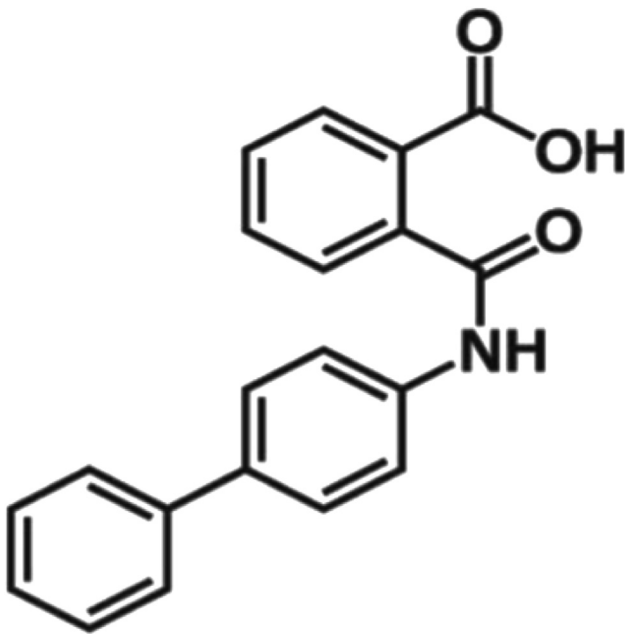


Fig 1. Chemical structure of kartogenin.

mesenchymal stem cells and tendon stem cells.^{6,7} The chondrogenesis induction properties of KGN have been investigated as a potential chondroprotective therapy for osteoarthritis^{6,8} and as a supplement to microfracture for the treatment of full-thickness cartilage defects.⁹ Recently, Wang et al.^{7,10,11} have studied the use of KGN, in combination with platelet-rich plasma (PRP), to facilitate fibrocartilage formation at the interface between tendon and bone, in an attempt to recreate the fibrocartilage zones of the native enthesis. In their studies, KGN treatment enhanced production of collagens I and II and increased expression of Sox-9 and scleraxis, consistent with the formation of fibrocartilage-like tissue.¹⁰ Additionally, KGN treatment resulted in more organized collagen fibers and chondrocytes at the tissue interface, and KGN-treated tendon–bone constructs demonstrated greater mean ultimate strengths compared with saline control.^{7,10} However, whether KGN can promote the formation of fibrocartilage-like tissue and/or improve the organization of collagen fibers within a healing rotator cuff tendon after its surgical repair is unknown. Augmentation of rotator cuff healing to generate a biomechanically stronger tendon-to-bone interface could result in substantial improvements in the functional outcomes of rotator cuff repair.¹²

The purpose of this study was to investigate the use of KGN in augmenting the healing of the repaired enthesis after rotator cuff repair in a murine model. The hypothesis was that KGN-treated animals would exhibit increased fibrocartilage formation, superior collagen fiber organization, and consequently, increased ultimate loads during biomechanical testing.

Methods

Study Overview

This study was approved by the Institutional Animal Care and Use Committee. A rotator cuff repair murine model was used. Each animal underwent unilateral detachment and transosseus repair of the supraspinatus tendon augmented with either fibrin sealant (control group; $n = 36$) or fibrin sealant containing KGN (experimental group; $n = 36$) applied at the tendon–bone repair site. Prior work has demonstrated that fibrin sealant itself does not improve tendon–bone healing in a rodent model of supraspinatus repair¹³; therefore, an untreated control group was not studied. The dependent variables were histologic measures of cellularity, fibrocartilage formation, and collagen fibril organization, as well as biomechanical tensile load-to-failure testing. Animals were humanely killed at 2 and 4 weeks for histologic and biomechanical analysis (Fig 2).

Preparation of KGN Beads

KGN (Sigma-Aldrich, St. Louis, Missouri) was dissolved in dimethyl sulfoxide (DMSO) at $15 \mu\text{g}/\mu\text{L}$ and added to fibrin sealant (Evicel Fibrin Sealant, Ethicon, Somerville, New Jersey) to obtain a final working concentration of $100 \mu\text{mol}/\text{L}$ KGN, a concentration used in prior studies.¹⁰ Therefore, each $7 \mu\text{L}$ of fibrin sealant bead contained $0.224 \mu\text{g}$ of KGN and $0.002 \mu\text{L}$ of DMSO. Similarly, control beads containing only DMSO and fibrin sealant were also prepared such

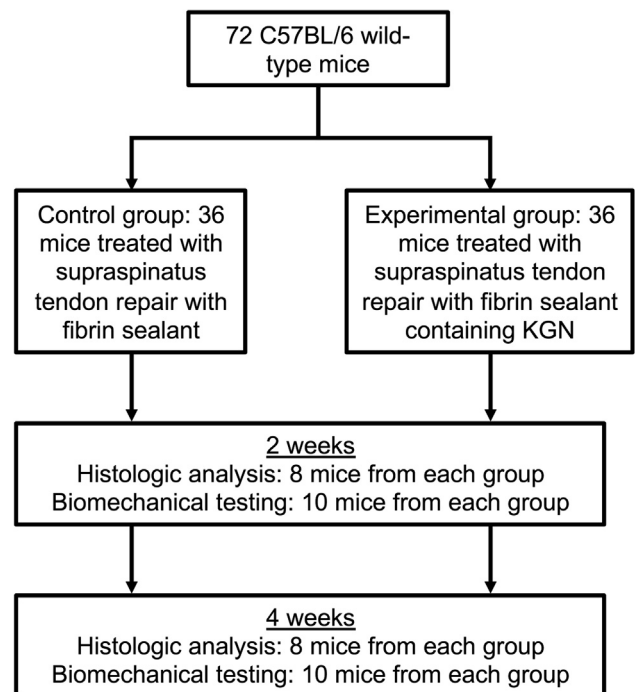


Fig 2. Flowchart of experimental protocol with control and kartogenin (KGN) groups.

that each bead contained an identical amount of DMSO present in each KGN bead (0.03% DMSO).

Surgical Procedure

Seventy-two skeletally mature (12 weeks old) male C57BL/6 wild-type mice (weight, 25-30 g) were used. A unilateral supraspinatus repair was performed using a previously described techniques.¹⁴ Briefly, after skin incision, the acromion was identified and elevated with a small hook. The deltoid was minimally detached to expose the rotator cuff tendons. The supraspinatus was isolated with an angled micro Adson forceps, and a 6-0 Prolene double-armed suture (Ethicon) was placed through the supraspinatus tendon using a modified Kessler stitch. The supraspinatus was then detached from its footprint on the humeral head, and the footprint was gently abraded using a scalpel. Two transosseous drill holes were created using a 30-G needle in a crossing configuration, one starting from the anterior aspect of the footprint and exiting the posterolateral cortex and other starting from the posterior aspect of the footprint and exiting the anterolateral cortex. The sutures limbs were then shuttled through each corresponding tunnel. Before tendon reattachment, fibrin sealant/DMSO (control group) or KGN suspended in fibrin sealant/DMSO (experimental group) was applied to the tendon–bone interface. The fibrin sealant bead was then secured and the tendon approximated by tying the sutures over the proximal humeral cortical bridge. The wounds were closed in a layered fashion. Postoperatively, animals were recovered with subcutaneous analgesic administration (buprenorphine, 0.05 mg/kg) and ad libitum cage activity.

In Vitro KGN Release

To quantify KGN release from the fibrin beads, KGN-fibrin gels (1 $\mu\text{g}/\mu\text{L}$) containing 250 μg KGN dissolved in 16.7 μL DMSO were prepared and suspended in 233.3 μL fibrin sealant. The gels were incubated in 0.5 mL phosphate-buffered saline (PBS) with 10% fetal bovine serum (FBS) at 37°C with continuous rotation using a micro-hybridization incubator for 7 days. The PBS solution was removed and replaced with fresh solution daily. Proteins were precipitated from the aliquoted PBS solutions with 1.5 mL acetonitrile, and the daily amount of KGN released from the gels was determined using liquid chromatography-mass spectrometry-mass spectrometry (Agilent Technologies, Santa Clara, California). The liquid chromatography method was a 2 mobile phase gradient (A = 0.1% formic acid in water; B = 0.1% formic acid in acetonitrile; solvents used were liquid chromatography/mass spectrometry grade and water was freshly drawn from a Milli-Q Integral system [Sigma-Aldrich]). The mobile phase ratio was 50:50 (A:B) for 1 minute and then 10:90 for 0.75 minute (total run time of 1.75 minutes); the injection volume was

1.0 μL , the column temperature was 40°C, and the flow rate was 0.6 mL/min. Concentrations for KGN release were calculated based on a KGN standard from 2 to 1000 nmol/L. This release experiment was performed 3 times with daily samples measured in triplicate.

Histologic Analysis

Eight animals in each experimental group were allocated for histologic analysis. Tissue specimens were fixed in 10% neutral-buffered formalin for 48 hours and then decalcified in Immunocal (Decal Chemical, Tallman, New York) for 24 hours. The tissues were then dehydrated, embedded in paraffin, and cut in 5- μm -thick sections in the coronal plane through the greater tuberosity and supraspinatus tendon. Serial sections were stained with hematoxylin and eosin, Alcian blue, and picrosirius red. Histologic sections were examined using light and polarized light microscopy (Eclipse E800, Nikon, Melville, New York) using a 10 \times objective, and digital images of the stained tissue sections were taken using a SPOT RT camera (Diagnostic Instruments, Sterling Heights, Michigan). The illumination and detection parameters of the microscope were kept constant between specimens to allow for direct comparisons.

Semiquantitative analyses for cell density, fibrocartilage area, and collagen fiber organization were performed using computerized image analysis with ImageJ software (National Institutes of Health, Bethesda, Maryland) within a standardized region of interest (e.g., repaired entheses). Cell density was quantified using manual thresholding with ImageJ and conversion of hematoxylin and eosin images to binary. Particle analysis was then performed to count the cells with the specific area. Percentage of fibrocartilage area at the repair site was identified with Alcian blue staining. First, the region of interest was manually outlined using ImageJ. Then, the percentage of Alcian blue–positive area within the outlined region of interest was calculated using a threshold of 0/120 in the red color channel.

Collagen fibril organization was evaluated with picrosirius red staining, and sections were illuminated with monochromatic polarized light. Bidirectional analysis was performed using a custom-made stage rotator. Photographs were taken of the repaired entheses at 0° (defined as the position where the long axis of the humerus is horizontal) and 45° of rotation. Mean signal intensity (brightness [B]) was quantified in gray scale for each of the 2 positions, and the change in brightness (ΔB) was measured by integrated density per micrometer squared was calculated. A higher ΔB indicates superior collagen fiber organization.¹⁵ All histomorphometric analyses were performed in a blinded fashion by 2 independent reviewers (Y.N., S.W.). The intraclass correlation coefficient (2,1) between the 2 reviewers was 0.81, 0.91, and 0.62 for cellularity, fibrocartilage, and collagen fiber organization analysis, respectively.

Biomechanical Testing

Ten animals in each experimental group were assigned to biomechanical testing to determine ultimate load and stiffness of the tendon–bone construct. At the 2- and 4-week intervals, the mice were humanely killed, and the supraspinatus–humerus construct was carefully harvested and stored at -80°C . Before testing, the specimens were thawed at room temperature and all soft tissue was dissected, preserving only the supraspinatus muscle–tendon–humerus construct. Additionally, all suture was removed. The humerus was potted in Bondo Filler (3M, St. Paul, Minnesota) in 2-mL tubes. Specimens were then mounted into a custom-designed materials testing system that allowed for uniaxial tensile loading at a 60° abduction angle. The tendons were first preconditioned for 3 cycles between 0.0 and 0.1 N and then loaded to failure at a rate of 1 mm/min. The ultimate load was recorded, and stiffness was calculated from the linear portion of the load–deformation curve. The site of failure (pullout from tendon–bone interface or tendon midsubstance) was also recorded.

Statistical Analysis

Previously published results on biomechanical testing of tendon attachment strength in similar rotator cuff repair rodent models were used for a power analysis.^{16,17} With those estimates, an a priori power analysis demonstrated that a sample size of 10 animals per group achieved 80% power to detect estimated effect sizes of 20% between 2 groups with 2-sided hypothesis testing. All data are presented as mean value \pm standard deviation of at least 3 replicates. The independent samples Student *t* test was used to compare results between groups at each time point. Significance was set at $P < .05$.

Results

All animals tolerated the surgical procedure. There were no perioperative complications. Animals in both groups resumed normal forelimb function and gait after recovery from anesthesia with no noticeable differences between the groups. There were no gross failures at the supraspinatus–greater tuberosity repair site in any of the 2- and 4-week specimens.

In Vitro KGN Release

Within the first 24 and 72 hours, $16 \pm 2\%$ and $22 \pm 2\%$ of the total KGN in the KGN–fibrin gel was released into the PBS-FBS solution, respectively (Fig 3). At 4 days, KGN release had plateaued, with $24 \pm 2\%$ of the total KGN dose released into the PBS-FBS solution.

Histomorphometric Analysis

At 2 weeks, hematoxylin and eosin staining demonstrated poorly organized, highly cellular, fibrovascular

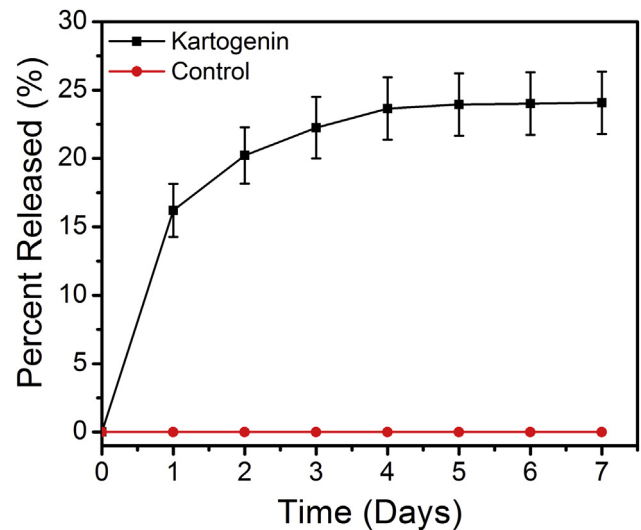


Fig 3. In vitro kartogenin (KGN) release: $16 \pm 2\%$ and $22 \pm 2\%$ of the total KGN in the KGN–fibrin gel was released into the phosphate-buffered saline–fetal bovine serum solution at 24 and 72 hours, respectively.

granulation tissue at the supraspinatus tendon–bone interface in both groups. Mean cell density was higher in the control group ($6,304 \pm 800$ cells/ mm^2) than the KGN group ($5,362 \pm 663$ cells/ mm^2) at 2 weeks ($P = .04$). At 4 weeks, remodeling of the initial granulation tissue had occurred, with areas of direct tendon–bone contact through a fibrovascular scar. In both groups, the interface remained highly cellular with new chondrocytes being more prevalent; however, they were not organized in any specific pattern. Mean cell density remained higher in the control group ($6,266 \pm 848$ cells/ mm^2) compared with the KGN group ($5,170 \pm 594$ cells/ mm^2) at 4 weeks ($P = .02$).

There was no difference in the mean percentage of Alcian blue–positive areas of fibrocartilage within the tendon–bone interface between the control group ($7.0 \pm 9.7\%$) and the KGN group ($5.1 \pm 10.9\%$) at 2 weeks ($P = .74$). However, at 4 weeks, the mean percent area of fibrocartilage at the tendon–bone interface was higher in the control group ($13.2 \pm 8.4\%$) than the KGN group ($4.4 \pm 5.4\%$; $P = .04$; Fig 4). The change in percentage of Alcian blue–positive areas from 2 to 4 weeks was not significant in either group.

There were no differences in collagen birefringence (ΔB) in the control group (12.9 ± 7.2 integrated density/ μm^2) compared with the KGN group (8.8 ± 3.6 integrated density/ μm^2) at 2 weeks ($P = .24$). In contrast, collagen birefringence was significantly higher in the KGN group (17.3 ± 2.0 integrated density/ μm^2) compared with the control group at 4 weeks (7.0 ± 6.5 integrated density/ μm^2 ; $P < .01$), indicating significantly more organized collagen fibers at the healing

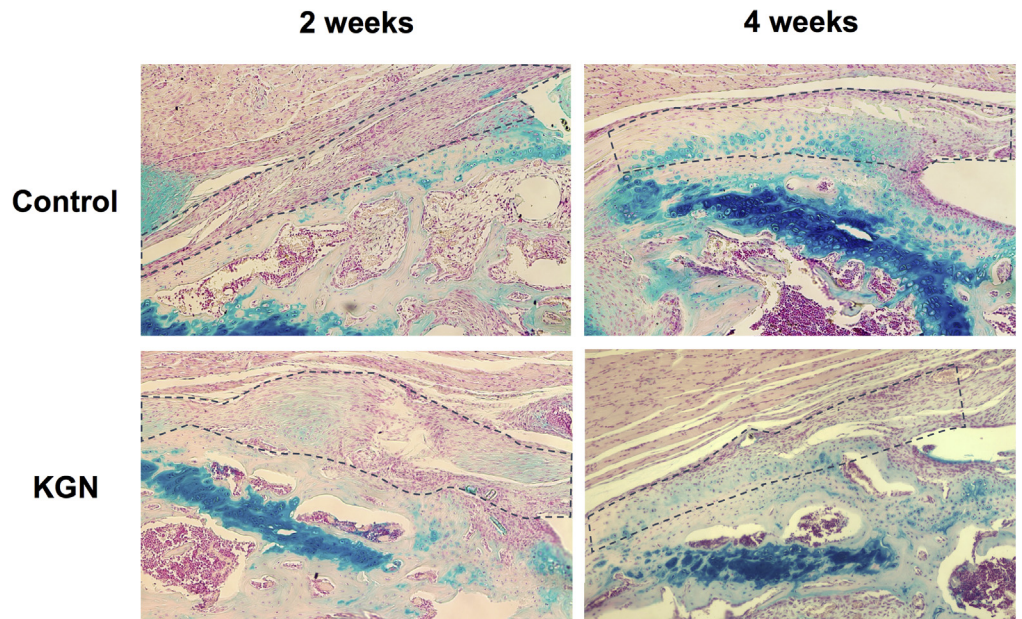
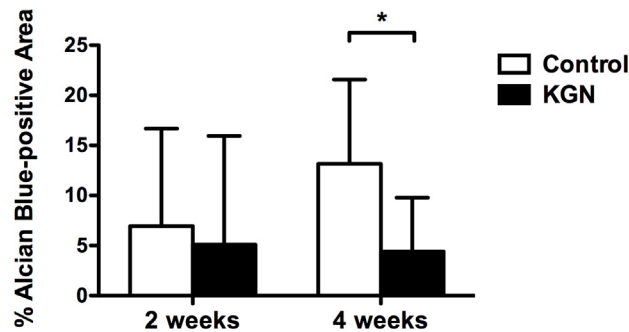


Fig 4. Percentage of Alcian blue-positive areas within the tendon–bone interface for the control and kartogenin (KGN) groups (original magnification $\times 10$). Area outlined by the dotted line represents the tendon–bone interface. $*P = .04$.



entheses (Fig 5). The change in collagen birefringence from 2 to 4 weeks was significant in the KGN group ($P = .01$), but not in the control group ($P = .14$).

Biomechanical Testing

At 2 weeks, there was no difference in the mean ultimate load between the control group (1.7 ± 1.1 N) and the KGN group (1.4 ± 0.3 N; $P = .27$). At 4 weeks, the mean ultimate load of the control group (2.3 ± 1.1 N) was significantly lower than the mean ultimate load of the KGN group (3.5 ± 0.6 N; $P = .04$; Fig 6). There were no differences in the mean stiffness between groups at 2 weeks (control group, 1.1 ± 0.34 N/mm; KGN group, 1.3 ± 0.3 N/mm; $P = .35$) and 4 weeks (control group, 1.6 ± 1.0 N/mm; KGN group, 1.2 ± 0.3 N/mm; $P = .25$). All specimens ($n = 40$) failed at the tendon–bone attachment site during load-to-failure testing.

Discussion

The principal findings of this study were that KGN-fibrin beads applied to the tendon–bone interface

in a murine model of rotator cuff repair resulted in an improvement in collagen fibril organization and biomechanical strength of the repaired enthesis at 4 weeks. Combined with the finding of lower cellularity, our data suggest that KGN leads to a more mature connective tissue microstructure at the healing enthesis.

Our results demonstrating enhanced collagen organization and superior biomechanical strength in KGN-treated tendon repairs are consistent with the results of 2 recent studies using KGN-PRP injection.^{10,11} Zhou et al.¹¹ compared the effects of KGN-PRP, PRP alone, or saline injection on tendon–bone healing within a bone tunnel in rats. At 8 weeks, the authors reported significantly higher pull-out strengths of the tendon graft from the bone tunnel in the KGN-PRP group compared with the PRP and saline control groups. Similarly, Zhang et al.¹⁰ compared the effects of KGN-PRP, PRP, and saline injection on healing in an Achilles punch biopsy rat model, and reported well-organized collagen fibers and mature chondrocytes aligning with the fibers at tendon–bone interface in the animals treated with KGN-PRP

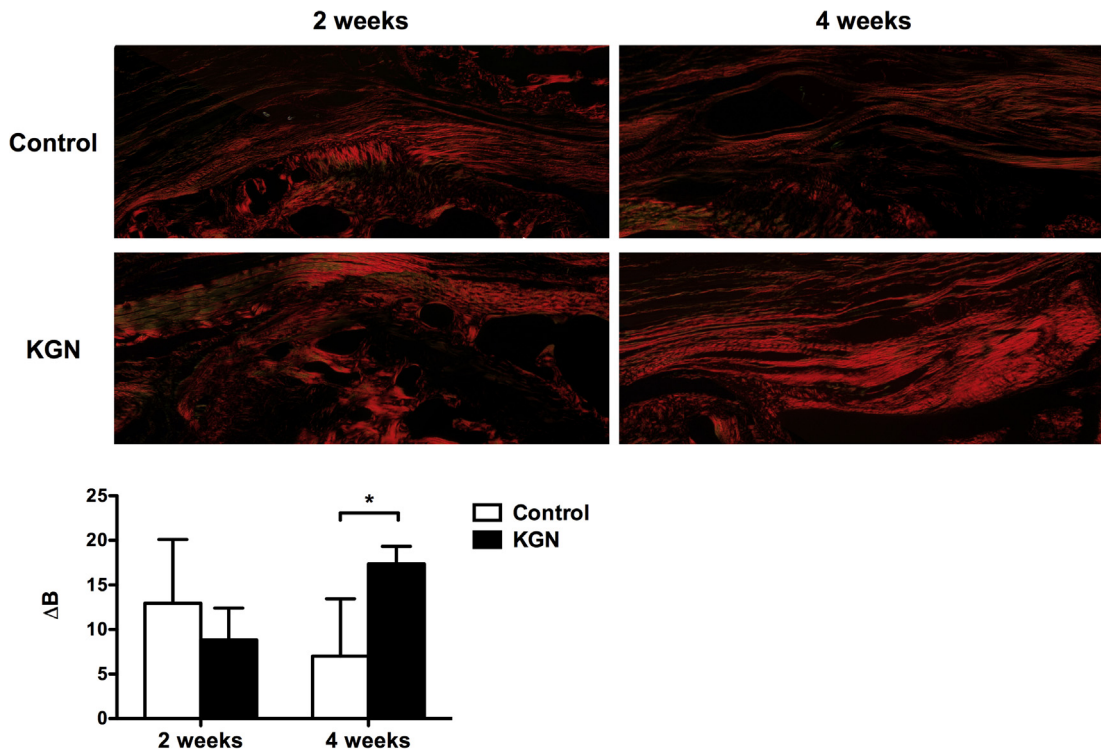


Fig 5. Collagen birefringence at the tendon–bone interface positioned at 0° for control and kartogenin (KGN) groups (original magnification $\times 10$). Collagen organization was measured by the change in brightness (ΔB) in gray scale between 0° and 45° of rotation. * $P < .01$.

injection. The PRP and saline-treated tendons demonstrated less-organized collagen fibers and a lack of chondrocytes. Moreover, the KGN-PRP–treated tendons demonstrated a greater mean ultimate tensile strength compared with the saline-treated tendons, consistent with the observation of persistent gaps in the wounds of the control tendons. Despite the lack of augmentation of cartilage-like tissue formation observed in our study, KGN treatment still seemed to enhance the formation and organization of collagen fibrils at the healing enthesis, which corresponds with its greater ultimate strength observed during mechanical testing.

The underlying cellular and molecular mechanism for the collagen structure-modifying effect in the surgically repaired tendon is unknown. This effect may be mediated through the CBF β -RUNX1 pathway or transforming growth factor- β /bone morphogenetic protein signaling,^{6,7,18} and warrants further investigation. Insight into this mechanism will help to optimize its delivery into the areas of the healing enthesis where the therapy is most needed. Of note, in their studies, Wang et al.^{10,11} discuss that their rationale for using a combination treatment of PRP and KGN relates to the numerous growth factors contained in PRP, along with the role of PRP gel as a carrier for KGN. PRP has been shown to stimulate cell proliferation, collagen production, and tenocyte differentiation of tendon stem cells,

thereby improving the remodeling of collagen fibrils of injured tendons.^{19–22} However, the authors did not investigate the effect of KGN alone in their studies, and whether a synergistic effect of PRP and KGN contributes to tendon-to-bone healing remains unknown.

Contrary to our hypothesis, we did not find more fibrocartilage formation in KGN-treated repairs, in contrast with results from other studies that describe the prochondrogenic effects of KGN in healing tendons. Zhang and Wang⁷ reported that KGN stimulates the proliferation and chondrogenic differentiation of bone marrow and tendon progenitor cells, as demonstrated by increased gene expression of aggrecan, collagen II, and Sox-9, as well as increased protein expression of proteoglycans, collagen II, and osteocalcin in cell

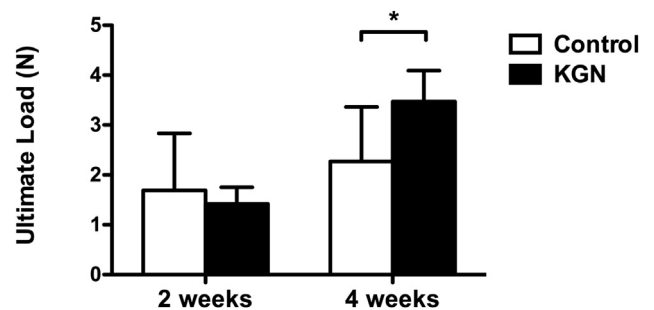


Fig 6. Mean ultimate load at 2 and 4 weeks for the control and kartogenin (KGN) groups. * $P = .04$.

culture. Additionally, in a biopsy punch injury model of the rat Achilles enthesis, injection of KGN induced formation of cartilage-like tissue in the wound, whereas injection of saline demonstrated no such response. A further study examined the effect of combined KGN and PRP injection in the same animal model and similarly reported histologic evidence of fibrocartilage formation in the wound.¹⁰ Immunohistochemical analysis showed abundant production of collagens I and II and increased expression of Sox-9 and scleraxis in KGN-PRP-treated tendons, confirming the formation of fibrocartilage, whereas a lower expression level of these fibrocartilage markers was found in the PRP and saline-treated tendons.

The chondrogenesis inductive properties of KGN have been used in animal models to mimic the structural changes seen in overuse tendinopathy,²³ augment microfracture for the treatment of full-thickness cartilage defects,⁹ prevent the progression of osteoarthritis,^{6,8} and induce the formation of meniscus-like tissue.²⁴ However, in our study, we found that KGN-treated animals had a lower percentage of Alcian blue-positive areas (indicating fibrocartilage formation) within the repaired enthesis compared with controls. There are several potential reasons for this discrepancy. First, our model differs from the Achilles punch biopsy model used by Wang et al. in that the supraspinatus tendon was fully transected at its footprint on the humerus before its transosseous repair. This model simulates an acute full-thickness supraspinatus tear that, without surgical repair, has little or no inherent capacity to heal. In a tissue that has a low inherent capacity to heal, an exogenous progenitor cell source may be needed for KGN to act on to stimulate chondrogenesis. Conversely, the Achilles tendon has a much greater healing potential, particularly in rodents,²⁵ owing to its extrasynovial nature where cells from the epitenon and tendon sheath can migrate and contribute to fibrous tissue formation after injury.³ Therefore, the application of KGN treatment for an Achilles injury may already be optimized owing to the abundance of progenitor cells at the repair site. Second, there is evidence to suggest that the molecular mechanisms by which KGN exerts its therapeutic effects are tissue specific. In articular cartilage, KGN was found to increase the expression of transforming growth factor- β Smads (Smad 2/3) while suppressing the bone morphogenetic protein Smads (Smad 1/5/8), thus inhibiting RUNX2. This inhibits the hypertrophy and terminal differentiation of chondrocytes, which is supportive of the chondroinductive effect of KGN.^{26,27} However, in human dermal fibroblasts, KGN increased type I collagen synthesis by activating the Smad 4/5 pathway.¹⁸ Further research is needed to delineate the cellular and molecular mechanisms by which KGN exerts its therapeutic effects, which may

differ depending on the specific tissue type. Third, in our study, KGN treatment resulted in slightly decreased cellularity at the healing enthesis compared with controls. It is unknown whether KGN has any inhibitory effects on cell chemotaxis or proliferation. Although we did not attempt to differentiate between cell types, a resultant decrease in the number of progenitor cells in an already relatively hypocellular tissue may contribute to the inability of KGN to induce the formation of cartilage-like tissues. Finally, the mechanical loading environment likely has an important effect on the actions of KGN, and the local biomechanical forces in the healing rotator cuff tendon are likely very different from Achilles tendon or from the intra-articular environment.

Although KGN treatment did not enhance fibrocartilage tissue formation in this animal model of rotator cuff repair, it did improve collagen fiber organization at the tendon-bone interface. The improved collagen fiber organization is likely a reason for the superior failure load of the healing enthesis,^{28,29} which validates the use of KGN to augment rotator cuff repair. Therapies that increase the formation of fibrocartilage tissue within the healing enthesis without improving the overall matrix organization may not necessarily improve the biomechanical strength of the tendon repair. Although rodent models generally exhibit more rapid and complete healing of tissues than the healing that occurs in humans, the use of this particular rotator cuff repair model allowed us to perform an initial screen of KGN application and to examine a proof of concept rather than to simulate a clinical scenario. Additionally, although the effects of a therapy may be more difficult to demonstrate owing to the rapid healing of small animal models, our results showed significant improvements in collagen organization and biomechanical strength with KGN. Much more research is needed into the cellular and molecular mechanisms by which KGN exerts its effect in various orthopaedic tissues. Improved understanding of these mechanisms will aid in determining when, where, and how much KGN to integrate into a therapy intended for enhancing rotator cuff repair.

Limitations

There are several limitations to this study. Although there seems to be a dose-dependent response to KGN,^{6,18} most in vivo studies, including this one, have only studied a single dose. Higher dosages or use of more optimized delivery systems may reveal different effects of KGN on rotator cuff healing in this specific model. Furthermore, regeneration of the 4 zones of the native enthesis likely requires more than just simple application of KGN at the surgical repair site. In our study, we continued to observe the generation of a fibrovascular scar at the tendon-bone junction, which

is biomechanically inferior and more prone to failure compared with the native 4-zone enthesis.^{30,31} Differential expression of numerous cytokines, transcription factors, and other signaling molecules at the healing tendon–bone enthesis that recapitulate the environment present during embryonic development is likely required to direct cell phenotype and promote the formation of the structure and composition of the enthesis.² Mechanical loading is critical to the processes of mineral accumulation, fibrocartilage formation, and collagen fiber formation that are intimately involved in a healing enthesis. However, as with most quadrupedal animal models, joint motion and loading on the healing tendon are difficult to control owing to the inability to reliably immobilize the extremity or restrict weight bearing.

Conclusions

Rotator cuff repair augmentation with KGN improved the collagen fiber organization and biomechanical strength of the tendon–bone interface at 4 weeks in a murine model.

References

- Hein J, Reilly JM, Chae J, Maerz T, Anderson K. Retear rates after arthroscopic single-row, double-row, and suture bridge rotator cuff repair at a minimum of 1 year of imaging follow-up: A systematic review. *Arthroscopy* 2015;31:2274-2281.
- Thomopoulos S, Genin GM, Galatz LM. The development and morphogenesis of the tendon-to-bone insertion: What development can teach us about healing. *J Musculoskelet Neuronal Interact* 2010;10:35-45.
- Thomopoulos S, Parks WC, Rifkin DB, Derwin KA. Mechanisms of tendon injury and repair. *J Orthop Res* 2015;33:832-839.
- Benjamin M, Toumi H, Ralphs JR, Bydder G, Best TM, Milz S. Where tendons and ligaments meet bone: Attachment sites ('enthesis') in relation to exercise and/or mechanical load. *J Anat* 2006;208:471-490.
- Rothrauff BB, Tuan RS. Cellular therapy in bone-tendon interface regeneration. *Organogenesis* 2014;10:13-28.
- Johnson K, Zhu S, Tremblay MS, et al. A stem cell-based approach to cartilage repair. *Science* 2012;336:717-721.
- Zhang J, Wang JH. Kartogenin induces cartilage-like tissue formation in tendon-bone junction. *Bone Res* 2014;2.
- Mohan G, Magnitsky S, Melkus G, et al. Kartogenin treatment prevented joint degeneration in a rodent model of osteoarthritis: A pilot study. *J Orthop Res* 2016;34:1780-1789.
- Xu X, Shi D, Shen Y, et al. Full-thickness cartilage defects are repaired via a microfracture technique and intra-articular injection of the small-molecule compound kartogenin. *Arthritis Res Ther* 2015;17:20.
- Zhang J, Yuan T, Zheng N, Zhou Y, Hogan MV, Wang JH. The combined use of kartogenin and platelet-rich plasma promotes fibrocartilage formation in the wounded rat Achilles tendon entheses. *Bone Joint Res* 2017;6:231-244.
- Zhou Y, Zhang J, Yang J, et al. Kartogenin with PRP promotes the formation of fibrocartilage zone in the tendon-bone interface. *J Tissue Eng Regen Med* 2017;11:3445-3456.
- Slabaugh MA, Nho SJ, Grumet RC, et al. Does the literature confirm superior clinical results in radiographically healed rotator cuffs after rotator cuff repair? *Arthroscopy* 2010;26:393-403.
- Schar M, Ma R, Sisto M, et al. *Fibrin glue does not improve rotator cuff healing in a rat model. Presented at the 10th Biennial ISAKOS Congress.* Lyon, France 2015.
- Lebaschi AH, Deng XH, Camp CL, et al. Biomechanical, histologic, and molecular evaluation of tendon healing in a new murine model of rotator cuff repair. *Arthroscopy* 2018;34:1173-1183.
- Lebaschi A, Deng XH, Zong J, et al. Animal models for rotator cuff repair. *Ann N Y Acad Sci* 2016;1383:43-57.
- Gulotta LV, Kovacevic D, Packer JD, Deng XH, Rodeo SA. Bone marrow-derived mesenchymal stem cells transduced with scleraxis improve rotator cuff healing in a rat model. *Am J Sports Med* 2011;39:1282-1289.
- Cohen DB, Kawamura S, Ehteshami JR, Rodeo SA. Indomethacin and celecoxib impair rotator cuff tendon-to-bone healing. *Am J Sports Med* 2006;34:362-369.
- Wang J, Zhou J, Zhang N, Zhang X, Li Q. A heterocyclic molecule kartogenin induces collagen synthesis of human dermal fibroblasts by activating the smad4/smads pathway. *Biochem Biophys Res Commun* 2014;450:568-574.
- Zhang J, Wang JH. Platelet-rich plasma releasate promotes differentiation of tendon stem cells into active tenocytes. *Am J Sports Med* 2010;38:2477-2486.
- Alsousou J, Thompson M, Harrison P, Willett K, Franklin S. Effect of platelet-rich plasma on healing tissues in acute ruptured Achilles tendon: A human immunohistochemistry study. *Lancet* 2015;385:S19 (suppl 1).
- Chen L, Dong SW, Tao X, Liu JP, Tang KL, Xu JZ. Autologous platelet-rich clot releasate stimulates proliferation and inhibits differentiation of adult rat tendon stem cells towards nontenocyte lineages. *J Int Med Res* 2012;40:1399-1409.
- Yu TY, Pang JH, Wu KP, Lin LP, Tseng WC, Tsai WC. Platelet-rich plasma increases proliferation of tendon cells by modulating Stat3 and p27 to up-regulate expression of cyclins and cyclin-dependent kinases. *Cell Prolif* 2015;48:413-420.
- Yuan T, Zhang J, Zhao G, Zhou Y, Zhang CQ, Wang JH. Creating an animal model of tendinopathy by inducing chondrogenic differentiation with kartogenin. *PLoS One* 2016;11:e0148557.
- Huang H, Xu H, Zhao J. A novel approach for meniscal regeneration using kartogenin-treated autologous tendon graft. *Am J Sports Med* 2017;45:3289-3297.
- Rodeo SA. Translational Animal Models in Orthopaedic Research. *Am J Sports Med* 2017;45:1487-1489.
- Decker RS, Koyama E, Enomoto-Iwamoto M, et al. Mouse limb skeletal growth and synovial joint development are coordinately enhanced by Kartogenin. *Dev Biol* 2014;395:255-267.
- Kempf H, Ionescu A, Udager AM, Lassar AB. Prochondrogenic signals induce a competence for Runx2 to activate hypertrophic chondrocyte gene expression. *Dev Dyn* 2007;236:1954-1962.

28. Gimbel JA, Van Kleunen JP, Mehta S, Perry SM, Williams GR, Soslowsky LJ. Supraspinatus tendon organizational and mechanical properties in a chronic rotator cuff tear animal model. *J Biomech* 2004;37:739-749.
29. Miller KS, Connizzo BK, Feeney E, Soslowsky LJ. Characterizing local collagen fiber re-alignment and crimp behavior throughout mechanical testing in a mature mouse supraspinatus tendon model. *J Biomech* 2012;45:2061-2065.
30. Apostolakis J, Durant TJ, Dwyer CR, et al. The enthesis: A review of the tendon-to-bone insertion. *Muscles Ligaments Tendons J* 2014;4:333-342.
31. Galatz LM, Sandell LJ, Rothermich SY, et al. Characteristics of the rat supraspinatus tendon during tendon-to-bone healing after acute injury. *J Orthop Res* 2006;24:541-550.

Submit to *Arthroscopy Techniques*

**Have you submitted your new
Technical Note and Video?**

Show your colleagues how you operate!

Submit at <http://ees.elsevier.com/arth/>